N O T I C E

THIS DOCUMENT HAS BEEN REPRODUCED FROM MICROFICHE. ALTHOUGH IT IS RECOGNIZED THAT CERTAIN PORTIONS ARE ILLEGIBLE, IT IS BEING RELEASED IN THE INTEREST OF MAKING AVAILABLE AS MUCH INFORMATION AS POSSIBLE

RADIAL EVOLUTION OF POWER SPECTRA OF INTERPLANETARY ALFVENIC TURBULENCE

B.Bavassano, M.Dobrowolny,
F.Mariani, N.F.Ness

IPS-81-13 September 1981

ISTITUTO
~~LABORATORIO~~ DI RICERCA E TECNOLOGIA
PER LO STUDIO DEL PLASMA NELLO SPAZIO
CONSIGLIO NAZIONALE DELLE RICERCHE
VIA G. GALILEI - FRASCATI

Radial evolution of power spectra of interplanetary Alfvénic turbulence

B. Bavassano[1], M. Dobrowolny[1,2], F. Mariani[2,1], N.F. Ness[3]

1) Istituto Plasma Spazio, CNR, Frascati (Italy)

2) Istituto di Fisica, Università di Roma, Rome (Italy)

3) Laboratory for Extraterrestrial Physics, NASA/GSFC, Greenbelt, Md (USA)

IPS-81-13 September 1981

Abstract

The radial evolution of the power spectra of the MHD turbulence within the trailing edge of high speed streams in the solar wind has been investigated with the magnetic field data of Helios 1 and 2 for heliocentric distances between 0.3 and 0.9 AU. In the analyzed frequency range ($2.8 \cdot 10^{-4} - 8.3 \cdot 10^{-2}$ Hz) the computed spectra have, near the Earth, values of the spectral index close to that predicted for an incompressible hydromagnetic turbulence in a stationary state. Approaching the Sun the spectral slope remains unchanged for frequencies $f \gtrsim 10^{-2}$Hz, whereas at lower frequencies we find a clear evolution toward a less steep falloff with frequency. The radial gradient of the power in Alfvénic fluctuations depends on frequency and it increases upon increasing frequency. For frequencies $f \gtrsim 10^{-2}$Hz, however, the radial gradient remains approximately the same. A discussion of possible theoretical implications of the observational features pointed out is given.

1. Introduction

Studies of power spectra of interplanetary Alfvénic turbulence date back to the discovery that this type of fluctuations is an important feature of the solar wind state (Coleman, 1968; Belcher and Davis, 1971), in particular present in the trailing edges of high speed streams. The early analysis of Coleman (1968) led to values of the spectral index of the power spectrum around 1.2 in the frequency range $(1 \cdot 10^{-4} - 1.3 \cdot 10^{-1})$Hz and first gave a discussion of these observations in terms of hydromagnetic turbulence theory.. In Belcher and Davis' work we find values of the spectral index between 1.5 and 2.2 in the frequency range $(1.5 \cdot 10^{-4} - 4 \cdot 10^{-2})$Hz. These and other works on the power spectrum of MHD fluctuations in the solar wind were put together by Russell (1972) who obtained and discussed a composite spectrum of this turbulence in the range $(1 \cdot 10^{-6} - 1)$Hz.

Other subsequent works, taking into account data at different heliocentric distances (for example using Pioneer 10 and 11 and Mariner 10 data), (Blake and Belcher, 1974; Behannon and Sari, 1977), have also considered how different features of these fluctuations vary with distance from the Sun. These results are reviewed in Behannon (1978). Most of these analyses were however considering long periods of observations referring to different solar wind regions and hence not necessarily homogeneous in relation to turbulence properties, i.e. affected also by perturbations other than the Alfvénic type.

More recently, the Helios interplanetary mission has allowed to study solar wind properties and their variations between the Earth's orbit and 0.3 AU. In particular, a very recent work by Denskat and Neubauer (1981), analyzing long periods of data containing hydromagnet-

ic turbulence, has indicated a quite interesting feature of the power spectrum. This is a variation of the spectral index of the power spectrum from values of $\sim$1 at 0.29 AU to values of $\sim$1.6 at 1 AU, in the overall frequency range considered (from $2.4 \cdot 10^{-5}$ Hz to $1.3 \cdot 10^{-2}$ Hz).

In this paper we present some new results on the power spectrum, also based on Helios 1 and 2 data, which further extend the work of Denskat and Neubauer.

The present analysis is different from theirs in two respects. The first is that it is based on periods as homogeneous as possible as far as the turbulence properties are concerned. In particular, we refer to periods of hydromagnetic fluctuations in the trailing edge of the same solar wind stream as seen by Helios 2 at three different heliocentric distances. We also include a period of Helios 1 data, on the same stream, at yet another distance and in a configuration where, at a given time, the two spacecraft were aligned on the same spiral magnetic field line (Villante, 1980). With our choice of periods we want to look at essentially the same turbulent region at different distances from the Sun. The second point of difference with respect to the analysis of Denskat and Neubauer (1981) is that, at each distance from the Sun, we perform a statistical study of the power spectrum differentiating between different frequency bands. As we will see, this will allow us to establish that a spectral index variation between 0.3 and 1 AU is actually occuring only for the low frequency region of the spectrum (frequencies $f \lesssim 10^{-2}$ Hz) whereas the higher frequencies (up to $f = 8.3 \cdot 10^{-2}$ Hz, which corresponds to the 6s. resolution of the data we have used) do not show any spectral index variations in the range of heliocentric distances covered by the data.

These results are on the same line of others we have recently obtained for different statistical properties of MHD fluctuations between 0.3 and 1 AU (Bavassano et al., 1981a). There we found that the radial gradients of several quantities, as power in the fluctuations, anisotropy in the plane perpendicular to the minimum variance direction, to depend from frequency but do not vary any more in the range of high frequencies.

In Sect. 2 of this paper we give a description of the analysis which has been performed. Sect. 3 contains our results on the power spectra of hydromagnetic fluctuations. The theoretical problems raised by these observations will be stated and discussed in Sect. 4.

2. Data analysis

For a description of the Helios orbits and the GSFC-University of Rome magnetometer experiment we refer the reader to Porsche (1977) and Scearce et al. (1975) respectively.

The periods considered in this analysis, their heliographic distance and latitude, their width in longitude are listed in Table 1 (where we give also the average field intensity and the corresponding proton gyrofrequency). The first three refer to Helios 2 data and are in the trailing edge of a high velocity stream observed by the spacecraft during three successive solar rotations at different distances from the Sun (0.87 AU, 0.65 AU and 0.29 AU respectively). The different durations of these periods were chosen in such a way that (taking into account the different rotational velocity of the Sun as seen from Helios) during each of them the spacecraft observes the same angular extent in

terms of heliographic longitude. Previous analyses (Bavassano et al. 1981a and b) have already established the homogeneity of these periods in their hydromagnetic fluctuation content and have been directed to a study of the polarization properties of the fluctuations and statistical properties other than power spectra analysis. In the second of the periods of Table 1 an opportunity to investigate the radial evolution of the turbulence in such a situation that slow temporal variations and heliographic latitude dependence cannot affect the results was offered by a favourable location of Helios 1 and Helios 2 spacecraft, which in this period were almost aligned along spiral magnetic field lines, at a distance from the Sun of 0.41 AU and 0.65 AU respectively and with a latitudinal separation of a few tenths of degrees (Villante, 1980). A period of Helios 1 data was therefore included in the analysis as indicated in Table 1. This was taken to correspond to that of Helios 2 in the sense of an equal angular extent in longitude and equal longitudinal separation from the end of the speed increase at the stream front.

Our estimates of the power spectra are obtained on the basis of 3h periods of 6s field averages through the usual technique of the cosine transform of the estimated correlation function (Blackman and Tukey, 1958). In each 3h period we obtain 300 estimates of the power spectrum, for all field components and the field magnitude, in the overall frequency range $(2.8 \cdot 10^{-4} - 8.3 \cdot 10^{-2})$Hz. This is therefore more extended in the high frequencies and less extended at low frequencies than the range of the recent analysis of Denskat and Neubauer (1981) (from $2.4 \cdot 10^{-5}$Hz to $1.3 \cdot 10^{-2}$ Hz).

Data gaps have been filled by linear interpolating the data immediately preceeding and following the gap. However the power spectrum

has not been evaluated when missing data overcome a given treshold.

Evaluation of noise sources (quantisation and instrument noise) shows that in the time intervals of interest the spectral densities of the magnetic field components exceed the estimated noise level in all the analyzed frequency range.

We have not attempted to separate the effect of static structures in the periods analyzed. It must however be remarked that the analysis of Bavassano et al. (1981b), referring to the same periods used in this study, has shown that the fluctuations verify quite strictly the condition B^2 = const ($\underline{B}$ being the total magnetic field) and can be considered as a mixture of purely perpendicular Alfvénic modes (rotational discontinuities would of course fit into this class) and modes which also contain a fluctuating component parallel to the average field. As for tangential discontinuities, of which some are certainly present in our data sample, we will discuss later their influence, if any, on our results.

3. Observational Results

In Fig. 1 we show average power spectra for magnetic fluctuations at the four different distances from the Sun quoted previously. Fig. 1a gives the total spectral density in components $P_C(f)$ (trace of the power spectral matrix), whereas Fig. 1b refers to the spectra $P_B(f)$ of fluctuations in field magnitude. The spectra which are plotted (one for each distance) are obtained by averaging, for each frequency, the values (at that frequency) obtained in all the calculated spectra at that distance. Individual spectra would show a similar behaviour with respect to the

curves reproduced in Fig. 1a and 1b with however more random fluctuations superimposed. We would note that our values for spectral densities satisfactorely fit with those by previous investigations at similar frequency and heliocentric distance ranges (see review by Behannon, 1978). The smoothing out operated by the averaging procedure makes more evident some general features. The most noticeable of these, looking at the spectra of total power of Fig. 1a, is the fact that, at small distances from the Sun, there is a clear flattening of the spectra in the low frequency region. This flattening decreases and then disappears for increasing distance from the Sun, the curves referring to distances of 0.65 and 0.87 AU being to a good approximation represented by straight lines (in the log-log scale) in all the frequency range considered.

Variations of the power spectra slopes with frequency are also recognizable in Fig. 1b referring to the compressible component of the fluctuations. As this component is very small (in comparison with total power), we limit ourselves here to the observation that the quite different behaviour of the curves for P_C with respect to those of P_B is indicative of the different nature of the compressible turbulent component. In the rest of the paper, although reporting some results also on fluctuations of field magnitude, we will concentrate especially on the spectra of total power, i.e. essentially the spectra of incompressible MHD fluctuations.

As usual, the power spectra obtained from the data for the magnetic field components are fitted to a power law $P_o f^{-\alpha}$ thus leading to a determination of the spectral index α. Doing that (for any magnetic component) for all our frequency range ($2.8 \cdot 10^{-4}$ Hz — $8.3 \cdot 10^{-2}$ Hz) we found only a slow variation of α with heliocentric distance, its average value going from ~ 1.65 at 0.87 AU to ~ 1.5 at 0.29 AU. This is in apparent contrast with the findings of Denskat and Neubauer(1981) who found in their frequency range ($2.4 \cdot 10^{-5}$ Hz — $1.3 \cdot 10^{-2}$ Hz) a varia-

tion of α from values ~ 1.6 at 1 AU to values ~ 1 at 0.29 AU. However, as it is already clear from the examination of the curves in Fig. 1a, if we evaluate our spectral exponent dividing our frequency range in two intervals, the first from $2.8 \cdot 10^{-4}$ Hz (our lowest frequency) to $1.3 \cdot 10^{-2}$ Hz (the high frequency limit of the computation by Denskat and Neubauer) and the second from $1.3 \cdot 10^{-2}$ Hz to $8.3 \cdot 10^{-2}$ Hz (our highest frequency), we obtain for the low frequency band essentially the same result of Denskat and Neubauer, whereas for the high frequency band we have $\alpha \sim 1.7$ quite independently from heliocentric distance. In other words, there is a radial variation of the spectral index depending from the frequency range and it is worthed to precise more carefully this dependence from the data.

For this we divided our overall frequency range into the intervals indicated in the first column of Table 2. The choice of these was made after several tests, with the criteria of obtaining both a sufficiently good resolution in frequency and a relatively small uncertainty in the determination of the spectral exponent. As seen from the Table, the frequency width of the intervals is different and increases in the high frequency bands, because at high frequencies the spectral index does not vary much with frequency (and thus we do not need a high resolution) while it does in the low frequency range.

For each of the computed power spectra the spectral index α was determined separately for the four frequency bands. Fig. 2 gives, at the various distances from the Sun, the distributions of the values of α for the z component of the fluctuations (in SE coordinates), the corresponding average values for each histograms being indicated by arrows. Following the histograms of a given column we obtain the variation of the spectral index distribution with distance for a given frequency band. It is then clearly seen that, for the lower frequency

intervals, in spite of a partial overlapping of the distributions, there is a real shift of the histograms of α with distance. In the first band for example, ($2.8 \cdot 10^{-4}$ Hz — $2.5 \cdot 10^{-3}$ Hz), we start at 0.29 AU with a distribution roughly centered around 1 (bottom of first column) and arrive near the Earth with a distribution shifted around 1.5 (top). Fig. 2 clearly shows also that this trend of variation disappears for the higher frequency bands. The same type of results, i.e. a definite radial gradient of the spectral index in the low frequency band and no variation for the higher frequencies, is also obtained from the analysis of the power spectra of the other components of the fluctuations. The average values of α as a function of frequency band and distance from the Sun have been reported in Table 2 (which also contains the spectral index values for $P_B(f)$).

Looking at the Table numbers we see that the deviations of α from the average values are of the same order of the variations of the averages with distance in the two lowest frequency bands. However, as seen from the histograms of Fig. 2, the variations of the average α values that we are talking about are very coherent and all in the same direction (see also the following Fig. 3) so that we are led to believe that the variation with frequency of the radial gradients of the spectral index α is significant.

A comprehensive view of the variation of the spectral index with frequency and heliocentric distance is shown in the drawing of Fig. 3, where we give a schematic representation of the average decrease with frequency of the spectral density for each of the four ensembles of power spectra obtained at the four heliocentric distances considered. Using for the spectral exponent the average values of Table 2, we have drawn, for the y component, an average spectrum by arbitrarly taking

equal to 10^3 the spectral density at the low frequency limit of our range and scaling with the frequency in the different bands on the basis of the corresponding spectral exponents. With these curves we have only the aim to give simple drawings showing the spectral index and its variation with frequency and distance, the values of the power density being completely arbitrary. It can be seen that the resulting spectra display a coherent variation with frequency and heliocentric distance. Near the Earth (lower curve) the overall spectrum shows an almost linear decrease with increasing frequency (in a log-log scale) with a spectral index close to 1.6 - 1.7, whereas approaching the Sun (upper curves) the slope is decreasing for decreasing frequency.

There is therefore an evolution of the power spectral index from 0.29 AU to 0.87 AU for the low frequencies ($f \lesssim 10^{-2}$ Hz) whereas for higher frequencies ($f \gtrsim 10^{-2}$ Hz) there seems to be essentially no variation. It should be noted that we found this type of variation also between the almost contemporary observations of Helios 1 at 0.41 AU and Helios 2 at 0.65 AU at the same heliographic latitude. This allows to exclude the possibility that changes in the spectrum are due to a slow evolution of the turbulence or to a dependence from heliographic latitude.

Finally we have evaluated, for each of the computed spectra, the average power density in each of the four frequency bands and looked for their radial gradient. In Fig. 4 we have plotted the mean values, for each distance and frequency band, of S_C, average power density in the magnetic field components (Fig. 4a), and of S_B, average power density in the field magnitude (Fig. 4b). Obviously the variation of the radial gradients of S_C with frequency, seen in Fig. 4a, is related to the behaviour of the spectral index discussed before. In our lowest frequency band it is found that S_C scales with distance about as r^{-3}. This

corresponds to having $\delta B^2 / \langle \underline{B} \rangle^2$ = const for these frequencies which, in the heliocentric range considered, represents and additional damping of the fluctuations with distance with respect to the variation corresponding to geometric optics propagation (δB^2 scaling as $\sim r^{-2.8}$ (Villante, 1980)). Notice that this same dependence of S_c ($\sim r^{-3}$) would be found also considering the average power in all our frequency range (on account of the greater weight of the low frequencies) in agreement with previous results of Behannon and Sari (1977) in the range (0.5 - 1) AU with Mariner 10 data. On the other hand we see from Fig. 4a that the radial variation of S_c referred to the higher frequency bands shows steeper gradients. For frequencies $f \gtrsim 10^{-2}$ Hz these radial gradients remain the same and correspond to a fall off of $\sim r^{-4}$ with radius.

For the compressible part of the fluctuations (Fig. 4b) the variation with frequency and radius is quite different than for S_c, indicating, as already seen from the power spectra, the quite different nature of this turbulent component with respect to the dominant incompressible part.

Finally the results of Fig. 4 agree with the ones obtained in a recent different type of work (Bavassano et al., 1981a), where a minimum variance analysis was done on the same set of data using different time basis for the statistics and, hence, for increasing time basis, including lower and lower frequencies in the samples. There a similar variation of radial gradients with frequency was found also for other parameters characterizing the fluctuations and, in particular, for their anisotropy in the plane perpendicular to the minimum variance direction. Our findings agree also with those of a recent work of Villante and Vellante (1981), which investigated, in various frequency

ranges, if the observed gradients in wave amplitudes were consistent with those expected from an undamped or from a saturated wave mode propagation.

4. Discussion

The essential feature of the above results is that they show a radial evolution of the power spectrum between 0.29 and 0.87 AU which precise the findings of Denskat and Neubauer (1981) by indicating that such evolution occurs only for the low frequency part of the spectrum ($f \lesssim 10^{-2}$ Hz) and is absent for higher frequencies. Although our sample did possibly contain some tangential discontinuities, we believe that the derived features reflect properties of the Alfvénic fluctuations. There are several arguments to support this view. The first is that one of the conclusions of earlier work on magnetic power spectra (Siscoe et al., 1968; Fisk and Sari, 1973), attempting to separate the contribution of directional discontinuities from that of MHD fluctuations is that the spectrum is dominated by such discontinuities only in the very low frequency region ($3 \cdot 10^{-5} - 3 \cdot 10^{-4}$ Hz), which is below our low frequency limit. Besides, from a simple model of directional discontinuities (Siscoe et al., 1968), one expects in our frequency range an f^{-2} behaviour of the spectral power due to discontinuities for observed values of their occurrence rate. The values of α that we found ($\alpha \lesssim 1.7$) throughout our frequency range are instead typical of an MHD spectrum. It seems therefore that the two main features of our results, i.e. radial variations of both average power density and spectral index which are frequency dependent, should be discussed in terms of properties of MHD turbulence in the solar wind.

Let us first discuss spectral index variations. Most of the values of α which we find in all our frequency range near the Earth's orbit and for frequencies $f \geq 10^{-2}$ Hz also at the other distances are in the interval 1.65 ± 0.15, close to the theoretical value $\alpha = 1.5$ predicted by Kraichnan (1965) for the inertial range of incompressible MHD turbulence in the stationary state (but also consistent with the Kolmogoroff 5/3 value for hydrodynamic turbulence).

On the other hand, in the low frequency part of our range ($2.8 \cdot 10^{-4} - 2.5 \cdot 10^{-3}$ Hz) we find values of α around 1 ($\alpha \sim 0.9 \pm 0.2$) at 0.29 AU and evolving toward the value 1.6 only upon approaching the Earth's orbit. A natural possibility to discuss is that the evolution is caused by non linear interactions still occurring in this low frequency part of the spectrum. Non linear interactions in Alfvénic turbulence, as shown in Dobrowolny et al. (1980a), occur between modes propagating in opposite directions with respect to the background magnetic field. Observations at 1 AU have repeatedly shown however (Belcher and Davis, 1971; Barnes, 1979) that most of the power is in waves of only one type. The same seems to be true also for the Helios data at the distances of closest approach to the Sun as it appears from the analysis of Denskat and Neubauer (1981) who selected data on the basis of definite and high correlation between velocity and magnetic field fluctuations (implying the dominance of only one type of waves). This is also actually confirmed by the fact that, as found here, fluctuations in field magnitude are very small and these fluctuations (Dobrowolny et al., 1980a) also depend from a non linear interaction between Alfvénic modes of opposite type.

Although from these arguments we must conclude that non linear interactions are quite weak, a future task of investigation should be

that of having a quantitative evaluation of such interaction and also that of investigating the effect of the small compressible part of the fluctuations on the dominant Alfvénic part.

Let us now consider the evolution of power in Alfvénic fluctuations with distance (see Fig. 4a). Our findings here (which are related to the evolution of the spectral index) are that the radial gradient of such power depends from frequency and it increases upon increasing frequency. For frequencies $f \gtrsim 10^{-2}$ Hz, however, the radial gradients seem to remain the same. This is in contrast with present ideas (see Hollweg, 1975 and Barnes, 1979, for reviews) on propagation of Alfvénic turbulence in the solar wind. Such propagation is usually described in the framework of geometric optics in which case, however, the radial gradients would not depend from frequency. Indeed, if we compare with the geometric optics approximation, which gives roughly a dependence $\sim r^{-2.8}$ for δB^2 in the range of distances considered (Villante, 1980), we find disagreement in all frequency bands considered and the disagreement increases with increasing frequency (see the $\sim r^{-4}$ dependence for $f \gtrsim 10^{-2}$ Hz).

It is very instructive to use our spectral analysis to obtain essentially the scale of the radial gradients as a function of frequency. This is done in Fig. 5 where we have reported, as function of frequency, the length λ corresponding to a damping in power levels of a factor e^2. The points in the figure are smoothed averages of the damping length values as obtained by evaluating, for every frequency, from the power densities of the average spectra of Fig. 1a, the additional reduction of the fluctuations with respect to the variation expected for geometric optics propagation (Hollweg, 1978). The solid line is only drawn to better visualize the variation of the damping length λ with

frequency. The value of λ remains practically unchanged at frequencies $f \geq 10^{-2}$ Hz. Uncertainties in λ are of the order of 15%.

This shows (even more clearly than the evolution of δ_c in Fig. 4a) that in order to interpret these results we seem to need a mechanism of damping increasing with frequency but flattening for frequencies $f \geq 10^{-2}$ Hz. As the present understanding of Alfvén waves (Hollweg 1975, Barnes 1979) is one where negligible damping mechanisms (both collisional and collisionless) are present, it seems that even on this point our observations open a not obvious theoretical problem.

Theoretical work is presently under progress to explain the observational features of power spectra we have pointed out here.

Acknowledgments

The magnetic data used in this paper are from the joint Consiglio Nazionale delle Ricerche/NASA experiments on Helios 1 and 2. We acknowledge discussions with P. Veltri and U. Villante.

REFERENCES

Barnes, A., Hydromagnetic waves and turbulence in the solar wind, in 'Solar System Plasma Physics', vol. I, ed. by E.N. Parker, C.F. Kennel, and L.J. Lanzerotti, p. 251, North Holland Pu. Co., 1979.

Bavassano, B., M. Dobrowolny, G. Fanfoni, F. Mariani, and N.F. Ness, Statistical properties of MHD fluctuations associated with high speed streams from Helios 2 observations, submitted to Solar Physics, 1981 a.

Bavassano, B., M. Dobrowolny, F. Mariani, and N.F. Ness, On the polarization state of hydromagnetic fluctuations in the solar wind, J. Geophys. Res., 86, 1271, 1981 b.

Behannon, K.W., Heliocentric distance dependence of the interplanetary magnetic field, Rev. Geophys. Space Phys., 16, 125, 1978.

Behannon, K.W., and J.W. Sari, Radial gradient of interplanetary magnetic field fluctuations from 0.5 to 1 AU, Eos Trans. AGU, 58, 486, 1977.

Belcher, J.W., and L. Davis, Large amplitude Alfvén waves in the interplanetary medium, J. Geophys. Res., 76, 3534, 1971.

Blackman, R.B., and J.W. Tukey, The measurement of power spectra, Dover, New York, 1958.

Blake, D.H., and J.W. Belcher, Power spectra of the interplanetary magnetic field, 0.7 - 1.6 AU, J. Geophys. Res., 79, 2891, 1974.

Coleman, P.J., Turbulence, viscosity and dissipation in the solar wind plasma, Astrophys. J., 153, 371, 1968.

Denskat, K.U., and F.M. Neubauer, Statistical properties of low frequency magnetic field fluctuations in the solar wind from 0.29 to 1.0 AU during solar minimum conditions: Helios 1 and Helios 2, submitted to J. Geophys. Res., 1981.

Dobrowolny, M., A. Mangeney, and P. Veltri, Properties of magnetohydrodynamic turbulence in the solar wind, Astron. Astrophys., 83, 26, 1980 a.

Dobrowolny, M., A. Mangeney, and P. Veltri, Fully developed anisotropic hydromagnetic turbulence in interplanetary space, Phys. Rev. Lett., 45, 144, 1980b.

Fisk, L.A., and J.W. Sari, Correlation length for interplanetary magnetic field fluctuations, J. Geophys. Res., 78, 6729, 1973.

Hollweg, J.V., Waves and instabilities in the solar wind, Rev. Geophys. Space Phys., 13, 263, 1975.

Hollweg, J.V., Some physical processes in the solar wind, Rev. Geophys. Space Phys., 16, 689, 1978.

Kraichnan, R.H., Inertial-range spectrum of hydromagnetic turbulence, Phys. Fluids, 8, 1385, 1965.

Porsche, H., General aspects of the mission Helios 1 and 2, J. Geophys., 42, 551, 1977.

Russell, C.T., Comments on the measurement of power spectra of the interplanetary magnetic field, Solar Wind, NASA Spec. Publ. 308, 365, 1972.

Scearce, C., S. Cantarano, N.F. Ness, F. Mariani, R. Terenzi, and L.F. Burlaga, Rome-GSFC magnetic field experiment for Helios A and B, NASA/GSFC Tech. Rep. X-692-75-112, 1975.

Siscoe, G.L., L. Davis, P.J. Coleman, E.J. Smith, and D.E. Jones, Power spectra and discontinuities of the interplanetary magnetic field: Mariner 4, J. Geophys. Res., 73, 61, 1968.

Villante, U., On the role of Alfvénic fluctuations in the inner solar system, J. Geophys. Res., 85, 6869, 1980.

Villante, U., and M. Vellante, Radial evolution of the IMF fluctuations: a comparison with theoretical models, submitted to Solar Physics, 1981.

s/c	time interval	heliocentric distance (AU)	heliog. latitude	heliog.long. interval	magnetic field intensity (nT)	proton gyro-frequency (Hz)
Helios 2	50 00:00 - 51 22:30	0.87	-6.6°	25.5°	6.8	0.10
Helios 2	76 00:00 - 78 00:00	0.65	-7.2°	25.2°	10.5	0.16
Helios 2	105 00:00 - 108 21:00	0.29	3.5°	25.1°	41.7	0.64
Helios 1	75 21:00 - 78 09:00	0.41	-6.9°	25.2°	23.0	0.35

Table 1 - Periods used in the analysis.

		(1)	(2)	(3)	(4)
	f(Hz) / R(AU)	$2.8 \cdot 10^{-4} - 2.5 \cdot 10^{-3}$	$2.5 \cdot 10^{-3} - 10^{-2}$	$10^{-2} - 3 \cdot 10^{-2}$	$3 \cdot 10^{-2} - 8.3 \cdot 10^{-2}$
B_{XSE}	0.87	1.60 ± 0.26	1.66 ± 0.24	1.71 ± 0.36	1.67 ± 0.21
	0.65	1.32 ± 0.22	1.62 ± 0.19	1.55 ± 0.27	1.81 ± 0.20
	0.41	1.22 ± 0.25	1.45 ± 0.24	1.63 ± 0.25	1.69 ± 0.18
	0.29	0.84 ± 0.25	1.25 ± 0.29	1.61 ± 0.22	1.72 ± 0.20
B_{YSE}	0.87	1.59 ± 0.30	1.63 ± 0.19	1.82 ± 0.20	1.78 ± 0.24
	0.65	1.32 ± 0.35	1.68 ± 0.23	1.72 ± 0.26	1.74 ± 0.19
	0.41	1.13 ± 0.34	1.41 ± 0.16	1.62 ± 0.24	1.78 ± 0.11
	0.29	0.89 ± 0.23	1.24 ± 0.27	1.73 ± 0.22	1.77 ± 0.19
B_{ZSE}	0.87	1.52 ± 0.19	1.66 ± 0.21	1.64 ± 0.29	1.70 ± 0.25
	0.65	1.36 ± 0.21	1.65 ± 0.31	1.53 ± 0.15	1.82 ± 0.17
	0.41	1.19 ± 0.16	1.45 ± 0.20	1.56 ± 0.18	1.78 ± 0.12
	0.29	0.95 ± 0.23	1.32 ± 0.26	1.69 ± 0.22	1.77 ± 0.20
B	0.87	1.81 ± 0.22	1.33 ± 0.40	1.25 ± 0.26	0.73 ± 0.38
	0.65	1.79 ± 0.22	1.35 ± 0.31	0.78 ± 0.37	0.56 ± 0.23
	0.41	1.57 ± 0.31	1.17 ± 0.39	0.75 ± 0.39	0.50 ± 0.28
	0.29	1.51 ± 0.37	0.96 ± 0.34	0.59 ± 0.22	0.28 ± 0.19

Table 2 - Mean values and deviations, as function of distance and frequency band, of the spectral index α for the magnetic field SE components and magnitude.

FIGURE CAPTIONS

Figure 1 - Average spectral densities, at the heliocentric distances given by R, of: (a) total power in components $P_C(f)$ (trace of power spectral matrix), (b) power in field magnitude $P_B(f)$. H1 and H2 are for Helios 1 and Helios 2 respectively.

Figure 2 - Histograms of the values of the spectral index α in different frequency bands (as given at the bottom) for the B_{ZSE} component. Arrows indicate the corresponding average values. H1 and H2 are for Helios 1 and Helios 2 respectively, R is the heliocentric distance, N the percentage of cases.

Figure 3 - Average falloff with frequency of the power density in the different frequency bands for the B_{YSE} component. Power densities are in arbitrary units. Each curve refers to a different heliocentric distance R. H1 and H2 are for Helios 1 and Helios 2 respectively.

Figure 4 - Variation with the heliocentric distance R, in different frequency bands, of: (a) average power density in the magnetic field components S_C, (b) average power density in field magnitude S_B. Numbers (1) to (4) indicate the frequency bands as labelled in Table 2 from low to high frequencies. For each curve we also give the slope of the corresponding best fit straight line.

Figure 5 - Damping length λ vs. frequency f. The smoothed curve is drawn only to better visualize the variation of λ.

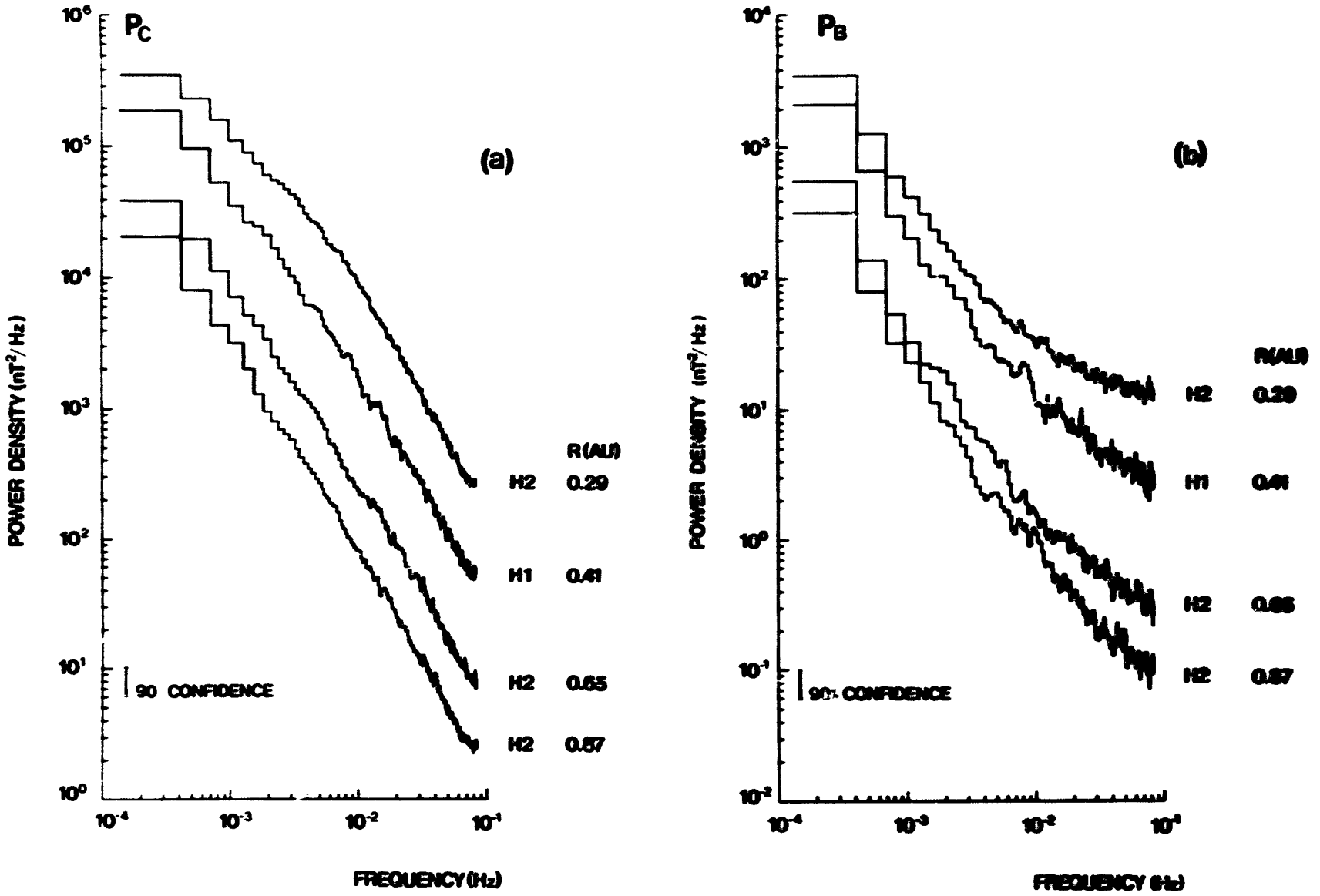
P_C
(a)
POWER DENSITY (nT²/Hz)
FREQUENCY (Hz)
R(AU)
H2 0.29
H1 0.41
H2 0.65
H2 0.87
90 CONFIDENCE
P_B
(b)
POWER DENSITY (nT²/Hz)
FREQUENCY (Hz)
R(AU)
H2 0.29
H1 0.41
H2 0.65
H2 0.87
90% CONFIDENCE

FIGURE 1

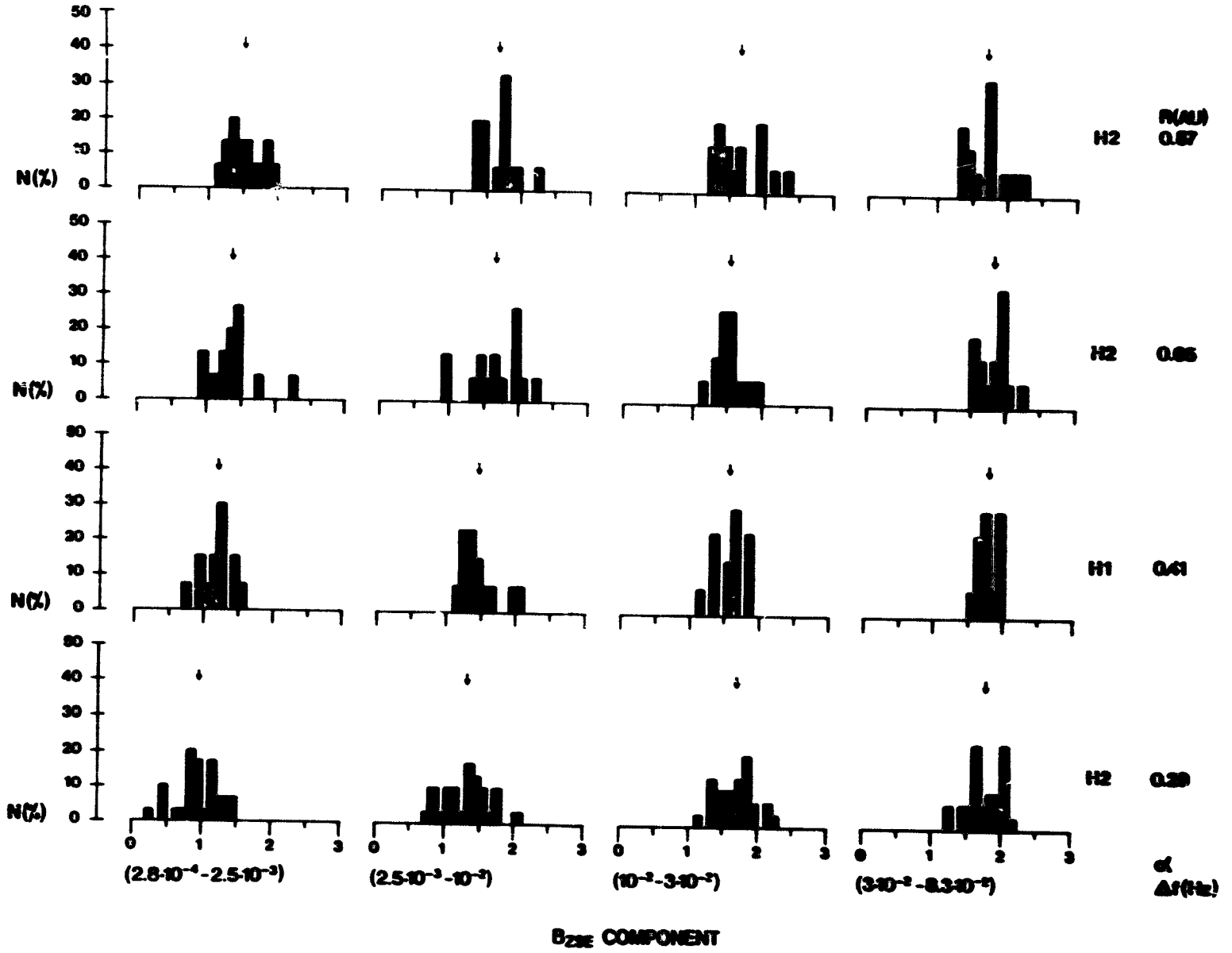
N(%)
H2
H2
H1
H2
P(ALI)
0.67
0.85
0.41
0.29
(2.8·10⁻⁴-2.5·10⁻³)
(2.5·10⁻³-10⁻²)
(10⁻²-3·10⁻²)
(3·10⁻²-8.3·10⁻²)
B₂₉₈ COMPONENT

FIGURE 2

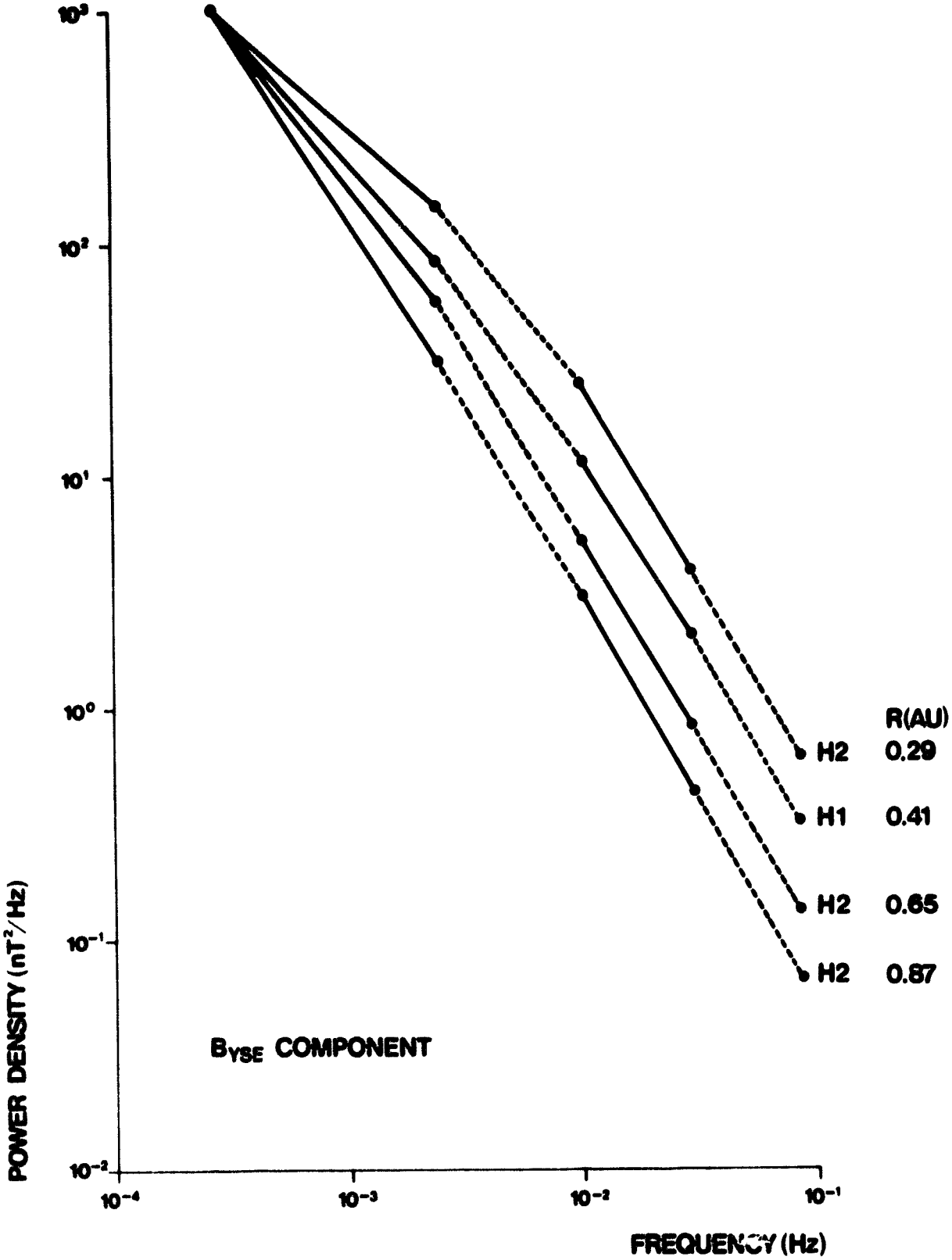
POWER DENSITY (nT²/Hz)
FREQUENCY (Hz)
B_YSE COMPONENT
R(AU)
H2 0.29
H1 0.41
H2 0.65
H2 0.87

FIGURE 3

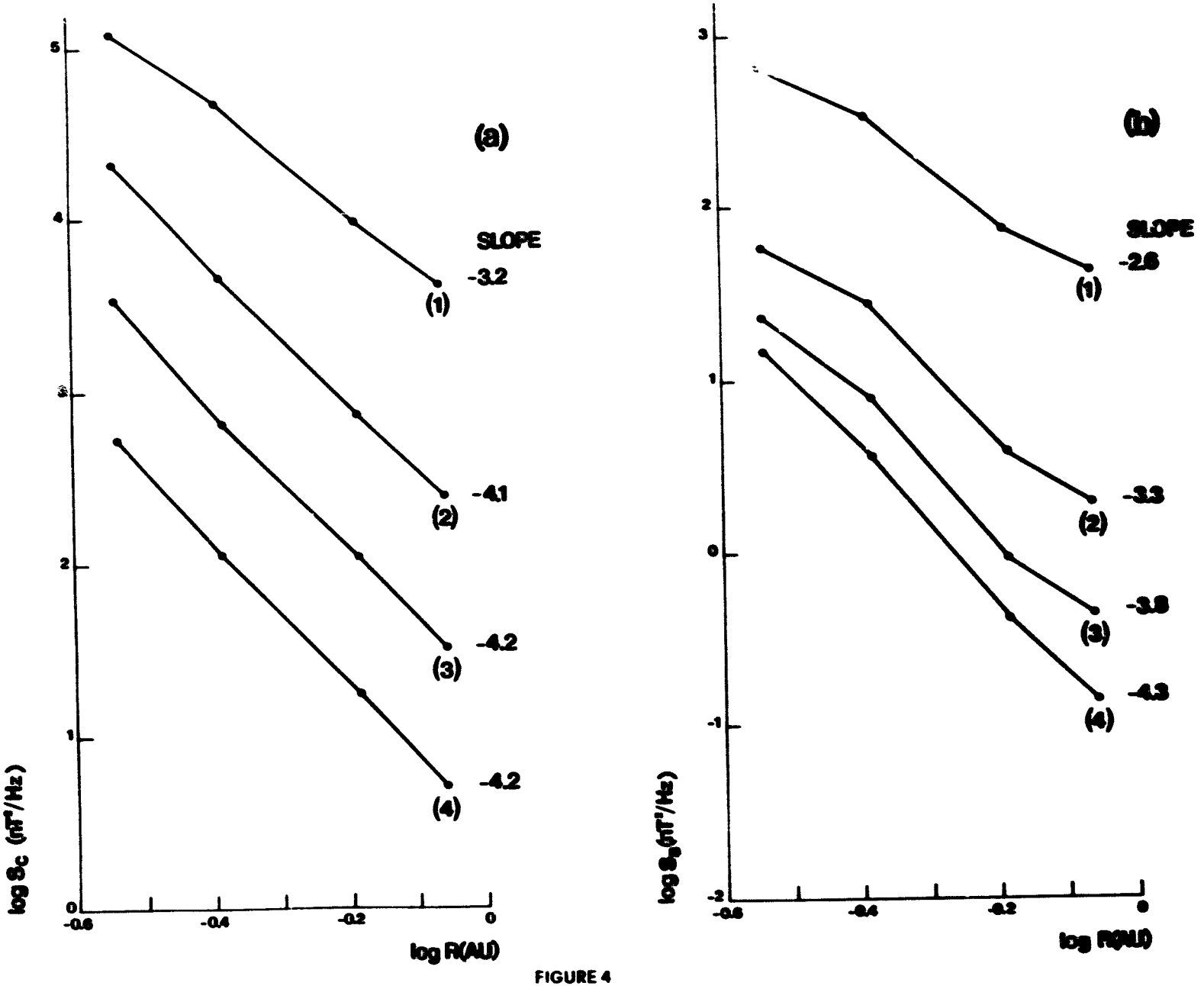
(a)
SLOPE
-3.2
(1)
-4.1
(2)
-4.2
(3)
-4.2
(4)
log S_c (nT²/Hz)
log R(AU)
(b)
SLOPE
-2.6
(1)
-3.3
(2)
-3.8
(3)
-4.3
(4)
log S_B(nT²/Hz)
log R(AU)

FIGURE 4

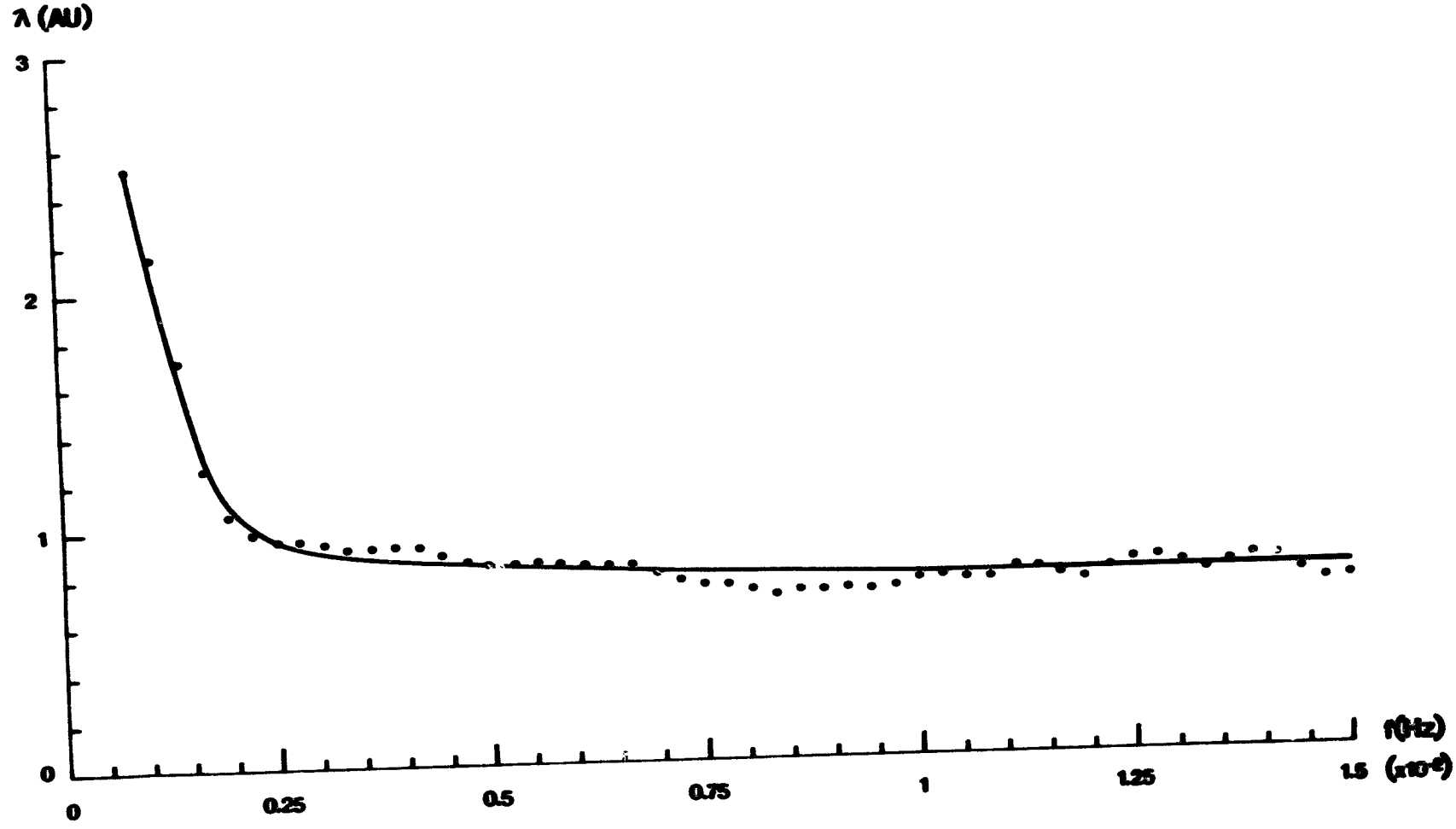

FIGURE 5